Water Air Soil Pollut (2013) 224:1710
DOI 10.1007/s11270-013-1710-2

Enhanced Transport and Transformation of Zerovalent Nanoiron in Clay Using Direct Electric Current

Helena I. Gomes · Celia Dias-Ferreira · Alexandra B. Ribeiro · Sibel Pamukcu

Received: 16 August 2012 / Accepted: 27 March 2013 / Published online: 20 November 2013

Abstract One of the major obstacles to zerovalent iron nanoparticles (nZVI) application in soil and groundwater remediation is the limited transport, especially in low-permeability soils. In this study, direct current (constant potential of 5.0 V) was used to enhance polymer-coated nZVI mobility in different porous media, including a bed of glass beads and kaolin clay. The tests were conducted using a modified electrophoretic cell and with nZVI concentrations typical of field applications (4 g L^{-1}). Experimental results indicate that the use of direct current can enhance the transport of the polymer-modified nanoparticles when compared with natural diffusion in low permeability or surface neutral porous medium. The applied electric field appeared to enhance the oxidation–reduction potential, creating a synergistic effect of nZVI usage with electrokinetics. Aggregation of the nanoparticles, observed near the injection point, remained unresolved.

Keywords Zerovalent iron nanoparticles (nZVI) · Enhanced transport · Direct current · Electrokinetics · Electrochemical treatment

Guest Editors: R Naidu, Euan Smith, MH Wong, Megharaj Mallavarapu, Nanthi Bolan, Albert Juhasz, and Enzo Lombi

This article is part of the Topical Collection on *Remediation of Site Contamination*

H. I. Gomes (✉) · S. Pamukcu
Department of Civil and Environmental Engineering, Fritz Engineering Laboratory, Lehigh University, 13 E. Packer Avenue, Bethlehem, PA 18015-4729, USA
e-mail: hrg@campus.fct.unl.pt

H. I. Gomes · A. B. Ribeiro
CENSE, Departamento de Ciências e Engenharia do Ambiente, Faculdade de Ciências e Tecnologia, Universidade Nova de Lisboa, 2829-516 Caparica, Portugal

H. I. Gomes · C. Dias-Ferreira
Instituto Politécnico de Coimbra, CERNAS – Research Center for Natural Resources, Environment and Society, Campus da Escola Superior Agrária de Coimbra, Bencanta, 3040-316 Coimbra, Portugal

1 Introduction

Zerovalent iron nanoparticles (nZVI) are a convenient and emergent remediation technology that could provide cost-effective solutions to soil and groundwater contamination (USEPA 2011). These nanoparticles have large surface areas for rapid uptake and transformation of a large number of environmental contaminants (Masciangioli and Zhang 2003; Li et al. 2006). Nanoparticles provide more flexibility for in situ applications than granular iron and can remain reactive for extended periods of time (>4–8 weeks) (Zhang 2003), showing characteristics of both iron oxides (sorbent) and metallic iron (reductant) (Sun et al. 2006). In field applications, the nanoparticle–water slurry has been injected under pressure and/or by gravity into the contaminated plume where treatment is needed; alternatively, nZVI can be transported by the flow of groundwater. However, in low porosity clay-rich media, it is challenging to achieve a uniform distribution of the slurry for effective remediation. Moreover, due to the relatively high ionic strength of most groundwater, favorable for colloidal

aggregation, bare nZVI has very limited mobility in the subsurface (Phenrat et al. 2007; Yang et al. 2007; Kanel et al. 2008; Bennett et al. 2010; He et al. 2010; Comba et al. 2011).

It is possible to use electric fields to effectively move nanoparticles through the soil. Some work has already been done to test this possibility, such as the one conducted by Pamukcu et al. (2008), in which polymer-coated nanoparticles were transported in kaolin by electrophoresis. Jones et al. (2010) also found that nZVI could be transported through fine-grained sand with rates comparable to those predicted by electrokinetic (EK) theory. More recently, modified or emulsified nZVI have been tested together with EK to treat dinitrotoluene (Reddy et al. 2011), trichloroethylene (Yang and Yeh 2011), and pentachlorophenol (Reddy and Karri 2009; Yuan et al. 2012) in spiked kaolin. Experiments with coarse and fine sand and sodium carboxymethyl cellulose stabilized nZVI showed that the electrophoretic enhancement in transport compared to diffusion was proportional to the applied current (Chowdhury et al. 2012).

The work presented here shows the advantages of direct electric current to overcome nZVI transport limitation while enhancing its activation in low permeability soils. Integrating both technologies, the role of direct electric current would be quite the opposite of the traditional one; instead of aiming at getting the contaminants out, it is used to get nZVI into the soil for in situ transformation and subsequent destruction of the contaminants. Bench-scale EK experiments in a modified electrophoretic cell were performed to investigate if the direct current enhances the transport and transformation of polymer-coated nZVI (Lin et al. 2010; Jiemvarangkul et al. 2011). A methodological and analytical approach including expeditious techniques to measure pH, electrical conductivity, oxidation–reduction potential (ORP), and iron content for determining the fate of nZVI in the soil was also developed and tested.

2 Experimental

2.1 Chemicals

Deionized (DI) water purged with ultra purified grade nitrogen gas (N_2) was used in all experiments. The purging was continued for at least 1 h so that the dissolved oxygen would fall to a level below 20 %. nZVI were prepared though the reduction of $FeSO_4$ $7H_2O$ (Fisher Chemicals) by sodium borohydride (Hydrifin^{TM}). The polymer coating of the nanoparticles was done using two different methods. For high concentration suspensions, bare nanoparticles were prepared and coated with polyacrylic acid, sodium salt—PAA Mw ~2,100 (Polysciences, Inc.) at 30 % following Jiemvarangkul et al. (2011). For the transport experiments, the freshly prepared suspension had a concentration of 4 g L^{-1} of nZVI, made using the one-step procedure described by Kanel et al. (2008). The particle size distribution of the nanoparticles had a mean value of particle diameter 62.66±39.6 nm and the median size was 60.2 nm (Jiemvarangkul 2012).

The electrolyte solution of 1 mM NaCl (Sigma Ultra) used in the electrode chambers was deoxygenated with N_2 for a minimum of 1 h before use.

2.2 Expedite Methods

Suspensions of different concentrations of PAA-nZVI (0, 0.0001, 0.001, 0.01, 0.1, 0.2, 0.5, 1, 2.5, 5, 10, 10, and 50 g L^{-1}) were prepared with 0.1 and 0.001 M solutions of NaCl with deionized water. Initially, the ORP, pH, and conductivity of these PAA-nZVI suspensions were measured with OAKTON bench-top meters at time steps of 0, 4, 12, 24, and 48 h. This data was used to generate calibration curves of relative nZVI concentration and reactivity. All the measurement probes (pH, conductivity, and ORP) were recalibrated before each measurement.

2.3 Electrophoretic Cell

A commercially available electrophoretic cell (EP) (Econo-Submarine Gel Unit, model SGE-020), originally designed for molecular separation, was modified to undertake these experiments (Fig. 1). The cell is a rectangular translucent box with a square (20 cm×20 cm) sample tray. There are two liquid chambers on each side of the sample tray (to hold the electrolyte reservoirs) and a lid that covers the whole apparatus. The standard cell is equipped with platinum working electrodes. Auxiliary electrodes and a reference electrode were added to the system for this experiment. The modified EP cell allowed direct measurement of the redox potential (ORP) in the test medium by use of 0.25-mm diameter platinum wire electrodes (auxiliary electrodes) fixed in the base plate of

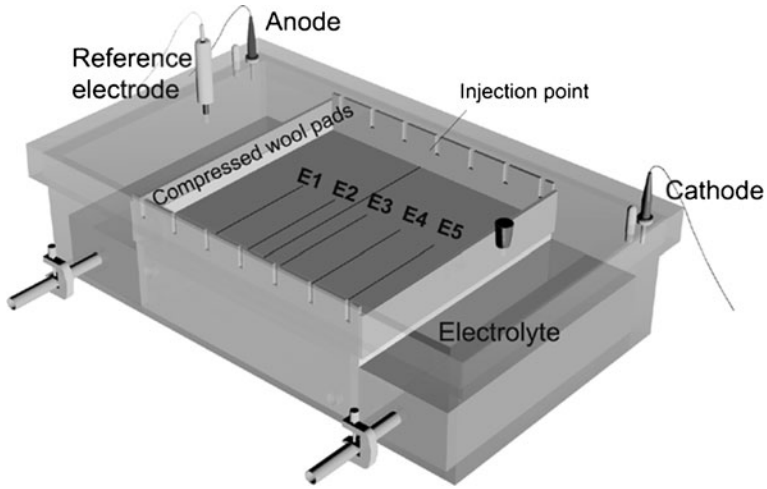

Fig. 1 Schematic diagram of the modified electrophoretic cell test setup

the sample tray at equal intervals (3 cm) with conductive glue. Redox potential measurements were made in the wire electrodes, using an Ag/AgCl reference electrode (Accumet) with 4.0 M KCl solution (Fig. 1). The auxiliary electrodes were labeled as E1–E5 starting from the anode electrode side of the tray (Fig. 1). An OAKTON pH probe (model WD-35805-18) was used for pH measurements in the test medium. Compressed fiberglass wool pads saturated and immersed in the electrolyte solutions on both sides of the tray were used to help transport the migrating ions from the electrolyte into the test medium and vice versa. The levels of the electrolyte liquids in the anode and cathode chambers were kept slightly below that of the test medium in the sample tray to avoid flooding, hence prevent preferential transport of nZVI through a water pool at the top. The experimental setup also includes a power supply, wiring, and a multimeter (Fluke 179).

2.4 Direct Current Enhanced Transport Experiments

Different porosity and surface reactivity test media, ranging from glass beads (with diameter less than 1 mm, previously sieved) to white Georgia kaolinite clay (>2 μm) were used in the enhanced transport experiments. Table 1 shows the various parameters of the experiments conducted in this study. A kaolin clay, previously characterized by Pamukcu et al. (2004), was used in this study. It was prepared to a final water content of 60 %, and the mixture had bulk mass density of 1.63 g cm^{-3} (Pamukcu et al. 2004).

The final pastes with different percentages of kaolin and glass beads were transferred to the tray of the electrophoretic cell and spread uniformly over the wire electrodes to an approximate thickness of 2 mm. PAA-nZVI were delivered using a syringe to inject 2 mL of its homogenized suspension through a tube and spreading it into a precut channel into the clay paste between the electrode ports E2 and E3 (Fig. 1).

A constant potential of 5.0 V was applied across the working electrodes for 48 h. This low potential was selected to remain within the linear range of the power supply used and also to prevent excessive gas generation. The constant potential of 5 V resulted in a current density in the range of 1.12 to 7.24×10^{-4} mA cm^{-2}. The cell was kept in a dark location to prevent iron photo-oxidation. Two sets of control experiments were conducted for each mixture under the same conditions, one without direct current application, and another with current but without the injection of PAA-nZVI.

Measurements were taken periodically at the following times: 0.25, 0.50, 0.75, 1, 2, 3, 5, 6, 7, 10, 12, 15, 24, 27, 32, 36, and 48 h. At each measurement, time voltage, current, ORP, and pH were monitored. At the end of each test, aqueous samples were collected from the electrode chambers, and composite solid samples were collected above the auxiliary wire electrodes E1-E5. The nZVI injection point was not sampled. The solid and aqueous samples were analyzed for total iron and ferrous iron concentrations. The iron was extracted from the matrix with the sodium dithionite-citrate-bicarbonate method (Mehra and Jackson 1960). The iron analyses were conducted using a PerkinElmer

Table 1 Enhanced transport experimental program and conditions

Test Number	Matrix	Moisture content (%)	PAAnZVI added (mL)	Average voltage (V)	Average current (mA)	Notes
1	Kaolin	60	2	5.043	0.27	Enhanced transport of nZVI
2	Kaolin	60	2	–	–	Diffusion control test
3	Kaolin	60	–	4.918	0.24	Control test without nZVI
4	50 % glass beads and 50 % kaolin	30	2	5.022	0.13	Enhanced transport of nZVI
5	50 % glass beads and 50 % kaolin	30	2	–	–	Diffusion control test
6	75 % glass beads and 25 % kaolin	30	2	5.097	0.10	Enhanced transport of nZVI
7	75 % glass beads and 25 % kaolin	30	2	–	–	Diffusion control test
8	100 % glass beads	20	2	5.110	0.27	Enhanced transport of nZVI
9	100 % glass beads	20	2	–	–	Diffusion control test
10	100 % glass beads	20	–	5.248 0	10	Control test without nZVI

AAnalyst 200 flame atomic absorption spectroscopy and a Hach DR 2800 spectrophotometer (UV).

3 Results and Discussion

3.1 Expedited Methods

The PAA-nZVI concentrations in DI water showed good fits to the linear regression analysis for conductivity for all, except for the measurements made at 12 h (Fig. 2). These curves did not change with the concentration of PAA-nZVI for either of the two concentrations of NaCl (0.001 and 0.1 M) in the suspension because the conductivity of NaCl completely masked the nZVI present. Hence, the conductivity could not be used as an expedite method to assess the distribution trends of the iron nanoparticles in the enhanced transport experiments.

There was no clear fit for the pH calibration curves in any of the tested suspensions, as the pH values measured at different concentrations of PAA-nZVI were identical and did not show meaningful changes in time (Fig. 3).

Since ORP measurements have been widely used as an indirect method to assess the results of injection of nZVI for groundwater remediation (Elliott and Zhang 2001; Henn and Waddill 2006; O'Hara et al. 2006), it was expected that these values could be used as a reliable indicator of nZVI concentration in the transport experiments. It was challenging to obtain stable values of the ORP for the suspensions tested, with some readings taking more than 30 min. The results showed that ORP decreased with increasing concentration of nZVI. The relationships between these variables were highly nonlinear, suggesting a complex response function that cannot be used reliably as a calibration curve (Fig. 4).

Examining the ORP variations in Fig. 4, the results for nZVI concentrations lower than 0.1 g L^{-1} suggest an approximately linear relationship (with R^2>0.90), consistent with a Nernstian dependence of this parameter on nZVI concentration. However, at higher concentrations, the ORP becomes relatively independent of the nZVI concentration. Both observations are consistent with the results of Shi et al. (2011) that used rotating disk electrodes in nZVI suspensions to assess the effects of nanoparticles on ORP. These researchers found that the response of ORP electrodes to suspensions of nZVI is not a simple function of iron nanoparticles concentration. At high concentrations of nZVI, ORP is dominated by direct interaction between the electrode and the nanoparticles, but this response is nonlinear and saturates with increased coverage of the electrode surface with adsorbed particles (Shi et al. 2011). At low nZVI concentrations, in aqueous suspensions, the measured ORP is a mixture of contributions that includes adsorbed nZVI and the dissolved H_2 and the Fe^{II} species that arise from corrosion of nZVI (Shi et al. 2011). Hence, the changes in ORP at low concentrations of nZVI

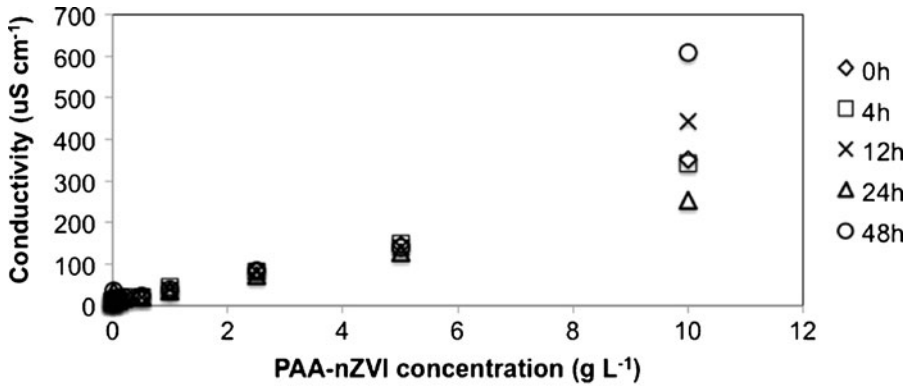

Time (h)	Linear regression	R^2
0	y = 33.161 x + 5.0706	0.9917
4	y = 32.471 x + 6.9457	0.9938
12	y = 26.88 x – 88.461	0.4722
24	y = 23.331 x + 15.328	0.9912
48	y = 53.488 x – 2.0660	0.9129

Fig. 2 Calibration curves for conductivity in deionized water

(<0.1 g L^{-1}) may be a viable method to track the relative spatial and temporal distribution of nZVI in controlled experiments.

3.2 Enhanced Transport of PAA-nZVI

3.2.1 Oxidation–Reduction Potential

The redox measurements in the kaolin during the experiments show the trend of oxidizing to reducing conditions from the anode towards the cathode when direct current is applied (Fig. 5). In general, the presence of clay appear to push the ORP up to more oxidizing conditions, while over time, the ORP values decreased, favoring reducing conditions in all samples. In the experiments with more percentage of glass beads, and in particular in the experiment with 100 % glass beads, there is an accentuated drop in the ORP values in the electrodes E1, E2, and E3 due to the injection and fast electrophoretic transport of PAA-nZVI in the absence of clay. The system attains equilibrium with more or less uniform and constant ORP

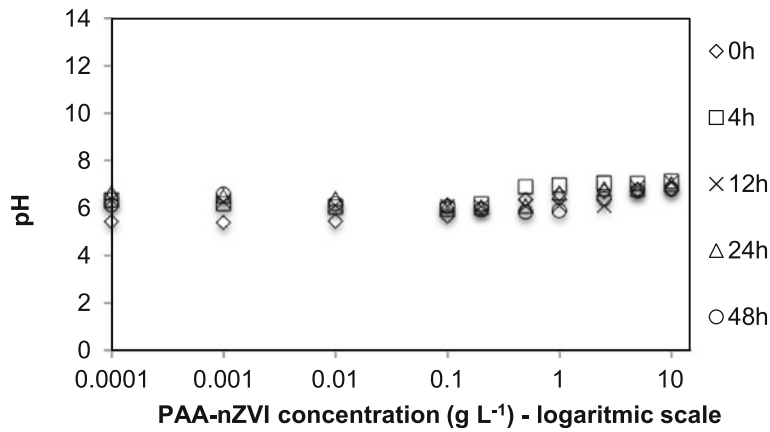

Fig. 3 pH values measured in the PAA-nZVI solution with 0.001 M NaCl

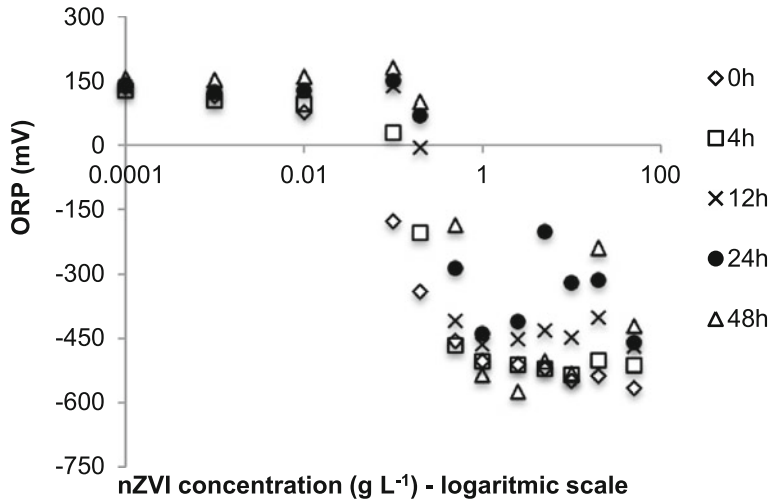

Fig. 4 ORP values measured in the PAA-nZVI solution with 0.1 M NaCl

after 15 h. In contrast, the presence of clay introduces a delay in ORP reduction possibly due to competing processes with iron reactivity such as sorption and electroosmotic transport of nZVI.

In the diffusion control experiments, the ORP values measured in all the electrodes (E1 to E5) showed little variation and are characteristic of oxidizing conditions (Fig. 6). In the glass beads experiment, the influence of the PAA-nZVI injection in both E2 and E3 is evident with a difference of more than 100 mV when compared to E1 and E4. In the experiments that included kaolin, this drop in ORP was not significant. Compared to the spatial and temporal distribution of ORP in the diffusion tests, the electric field enhance the spending of the nZVI through faster transport and activation, while presence of clay delay both processes.

3.2.2 pH

The initial pH in the different experiments varied from 4.05 to 4.85 when kaolin was present and from 5.40 to

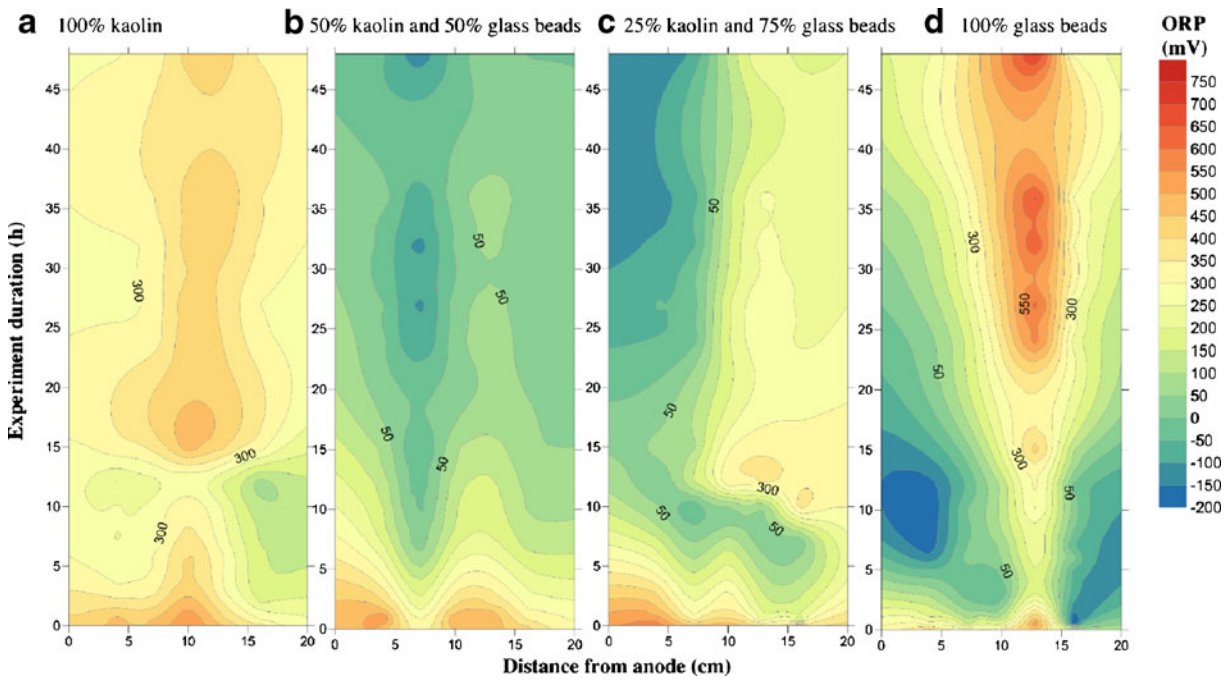

Fig. 5 ORP values measured at the auxiliary electrodes during the enhanced transport of nZVI tests in the different porous materials

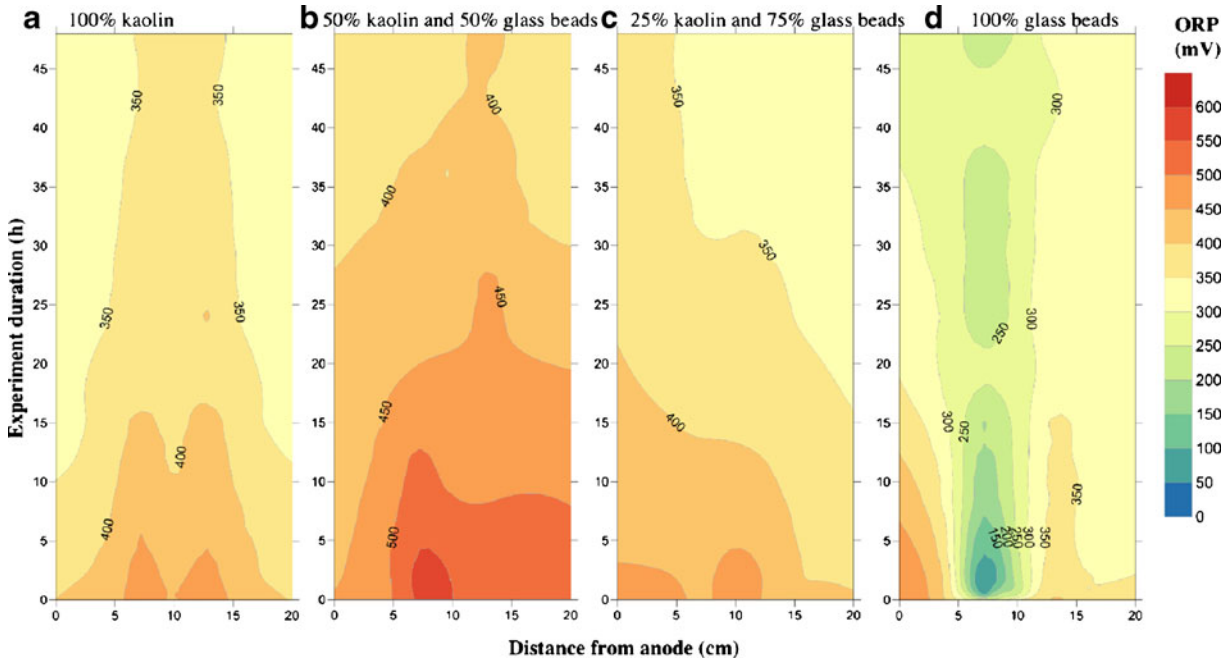

Fig. 6 ORP values measured in the electrodes during the diffusion tests in the different porous materials

7.19 in the experiments with 100 % glass beads (Fig. 7). This pH is favorable to the nZVI oxidation. Other researchers have observed that low pH increases deposition of nZVI in clay, as well as nZVI aggregation (Kim et al. 2012). Therefore, the initial conditions in the matrix were not advantageous to the mobility of PAA-nZVI. The pH values measured during the experiments showed some fluctuation, with values between 3 and 5.52, when some percentage of kaolin existed in the matrix. The typical profile of a pH front increasing from the anode to the cathode in electrokinetic treatments was not observed in these tests (Fig. 7). This outcome can be attributed to the low values of current density applied, the absence of the physical conditions for fast transport of H^+ and OH^- from the electrode compartments into the media, and possibly the presence of iron that kept the pH low at the cathode side. Only in the experimental setups with 100 % glass beads was the effect on pH from the injection of the PAA-nZVI noticed, particularly in E2, E3, and E4, where pH values higher than 8 were measured.

Normally, due to the electrolysis of water in the electrode compartments that produce H^+ ions at the anode and OH^- ions at the cathode, the final solution pH values would approach values around 2 and 12, respectively. The values observed in the experiments (Fig. 8) varied between 2.71 and 11.03 and are consistent with those electrochemical reactions of water electrolysis. In the diffusion experiments, a small decrease in the pH in both anode and cathode compartment was observed. A possible explanation is the increase in H^+ in solution due to the oxidation of Fe^0.

3.2.3 Iron-Enhanced Transport

Since PAA-coated nanoparticles have negative zeta potential and tend to electrophoretically transport towards the anode (Yang et al. 2008), some of the earlier preliminary experiments were conducted with the injection point located near the cathode (results not shown). In those experiments, it was observed that the electroosmotic flow (EOF) was counterbalancing the electrophoretic transport of the nZVI. This is consistent with the predictions of Jones et al. (2010) that the EOF rates will increase, due to the large apparent zeta potentials existent in natural clays, counteracting electrophoresis and reducing the overall migration rate of nZVI when compared with diffusion. Other researchers also tested different injection points in electrokinetic experiments to enhance nZVI transport. Experimental results showed that the cathode reservoir was the most unsuitable injection spot, due to the alkaline environment that promotes the formation of iron oxides at the surface on nZVI (Yang et al. 2008;

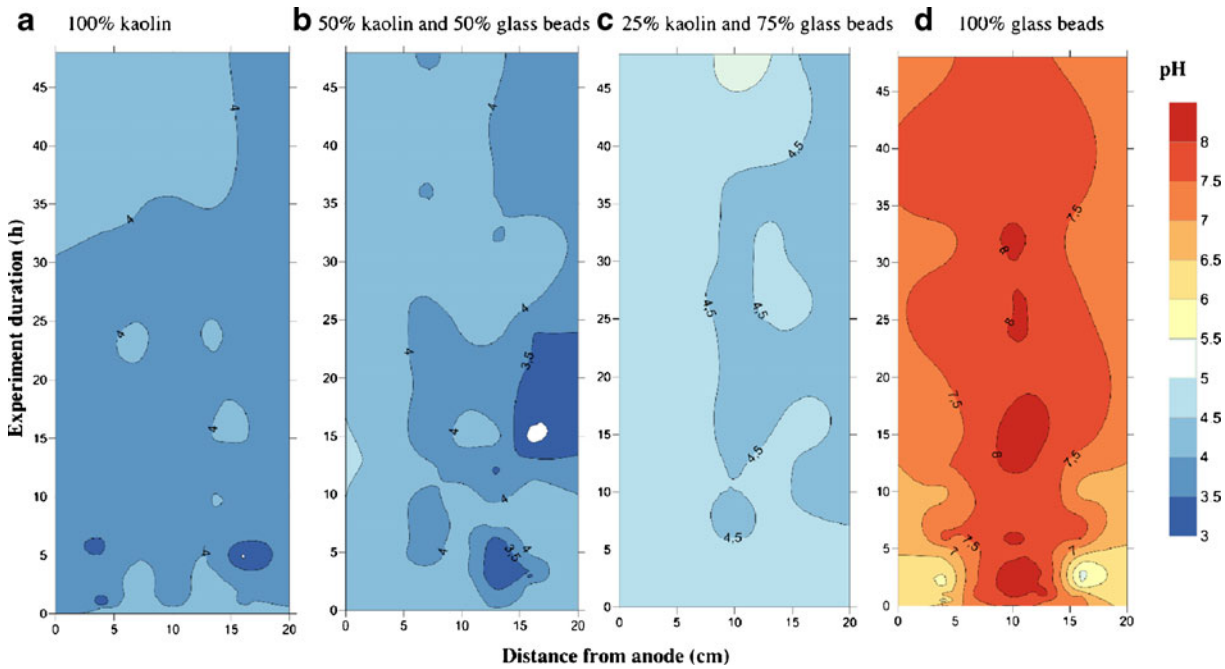

Fig. 7 Variation of pH in the matrices tested during the experiments

Yang and Yeh 2011). On the other hand, it was also found that corrosion on nZVI was higher when injected in the anode compartment, due to increased dissolved oxygen and lower pH (Chang and Cheng 2006; Chowdhury et al. 2012). Based on the observations of the preliminary tests conducted and the results available in the literature, the injection point used in the experiments was selected in the central area of the EP

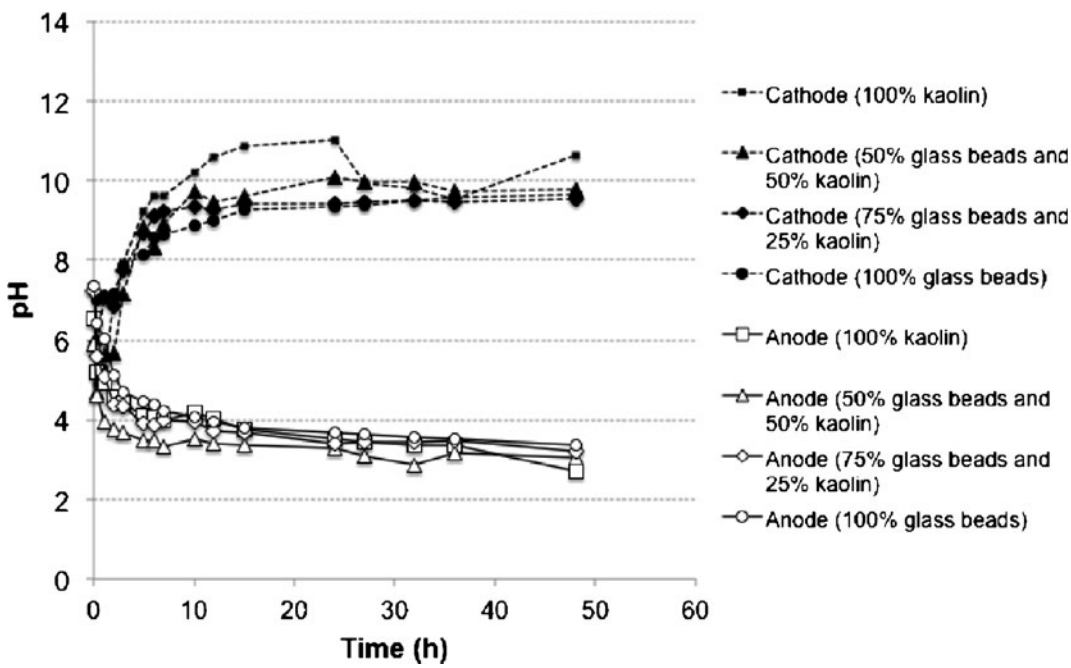

Fig. 8 Variation of pH in the cathode and anode compartments during the enhanced transport experiments

cell (between E2 and E3), to avoid rapid corrosion of the nZVI by extreme pH conditions and be able to discern the controlling transport mechanism of the nanoparticles (i.e., electrophoresis towards the anode or electroosmosis towards the cathode).

Figure 9 shows the total iron distribution in the electrophoretic cell at the end of the experiments and compares the direct current enhanced transport with diffusion. In general, there are higher concentrations of iron across the test bed when direct current is applied. It is also clear that higher concentrations near the cathode (E5) are only obtained when the matrix has higher percentage of kaolin, reflecting the importance of EOF. In all the experiments with glass beads, there is a very well-defined peak of concentration at E3 (i.e., practically the injection point). This is potentially due to the aggregation or fast corrosion of the iron nanoparticles, or to both phenomena. It has been previously shown that at high particle concentrations (1–6 g L^{-1}), there is a higher tendency for agglomeration (Phenrat et al. 2009). When nZVI aggregate and form agglomerations larger than the soil pores, their transport becomes restricted (Reddy et al. 2011). There can also be changes to the mobility of nZVI due to volumetric expansion with corrosion. The volume of corrosion products (Fe hydroxide or oxide) is larger than that of the original metal (Fe^0), and these products are likely to contribute to porosity loss and also promote particle agglomeration (Noubactep et al. 2012).

According to Bahranowski et al. (1993), Fe may be present in kaolinite as a part of its structure or as separate Fe-rich phases. Usually, both types of contamination, referred to as "structural" and "nonstructural", or "free" iron, coexist in kaolinite. In the former case, Fe may either substitute for Al in the octahedral gibbsite [$Al(OH)_3$] sheet or Si in the tetrahedral Si-O skeleton. In the latter, it belongs to separate Fe-rich phases such as Fe-bearing micas or iron oxides/oxyhydroxides (Bahranowski et al. 1993). The lower concentrations of Fe in the experiment with 100 % of glass beads when compared to those with kaolin might be explained by Fe impurities present in the kaolin. In fact, the blank samples with the same percentages of kaolin and glass beads showed background iron concentrations directly proportional to the percentage of kaolin present in the matrix.

It was also observed that PAA-nZVI did not move into the water phase in the electrode chambers, except for the cathode chamber in the enhanced transport tests with 100 % kaolin (final concentration of 0.43 mg L^{-1}) and 100 % glass beads (0.74 mg L^{-1} in the anode compartment and 0.09 mg L^{-1} in the cathode). This indicates that EOF was dominant in transporting nZVI in pure clay,

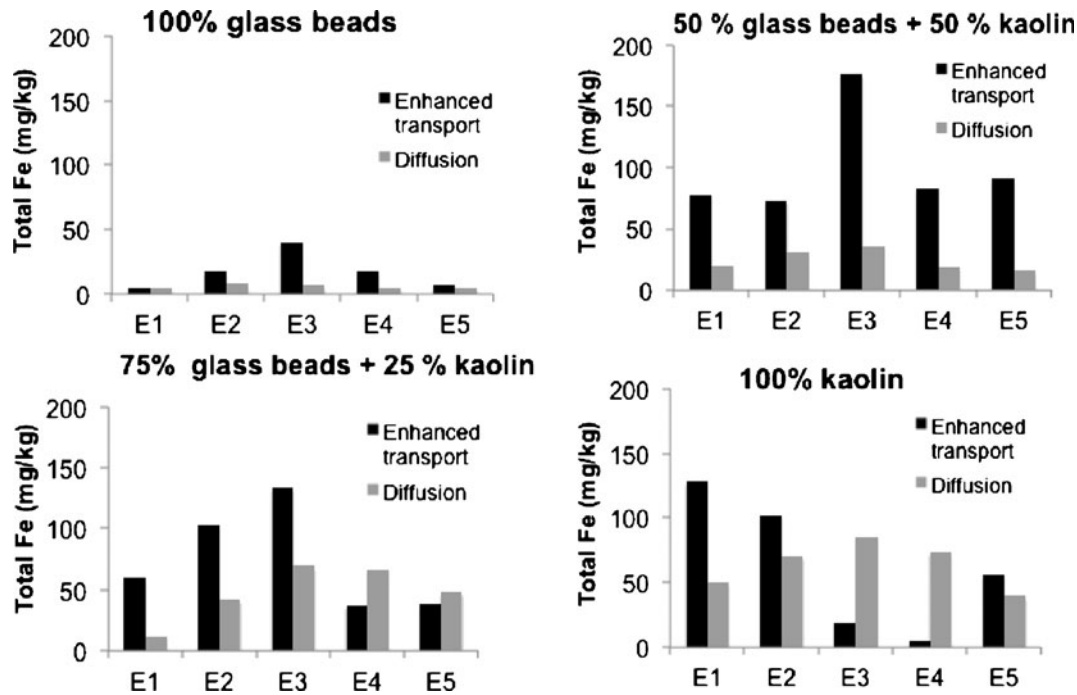

Fig. 9 Total iron distribution on the electrophoretic cell

while electrophoresis was the only mechanism to transport nZVI in surface neutral glass beads. In mixed samples, it appears that EOF and electrophoresis competes, resulting in prolonged presence of iron in the pores and potential capture on the clay surfaces. Other experimental results showed that there was greater deposition of nZVI onto clay minerals compared to similar sized silica fines due to charge heterogeneity on clay mineral surfaces (Kim et al. 2012).

3.2.4 Iron Oxidation State

All oxidation–reduction potentials measured in the electrodes across the electrophoretic cell were referenced to the normal hydrogen electrode by subtracting the potential of the Ag/AgCl reference electrode. These values combined with pH values allowed the construction of a Pourbaix (Eh–pH) diagram, showing the potential oxidation states of the iron (Fig. 10). Since predictions from stability diagrams are only accurate when the system approaches thermodynamic equilibrium in aqueous solutions, the plot is only intended to give an indication of the dominance of particular Fe species at the recorded Eh and pH measurements. In this diagram, all data from diffusion tests form a cluster that corresponds to the formation of Fe_2O_3 under oxidizing conditions (passivity region). Regarding the experiments with direct current enhanced transport of PAA-nZVI, the values measured above E1 and E2 electrodes (i.e., nearest to the anode), during the first 6–7 h of the experiments, match the Fe^{2+} area (corrosion region). There is a very distinct cluster of values measured in the glass beads bed, where pH values were much higher than in other experiments. These results are consistent with the visual observations of the iron injected in the cell, since only after 1 h, it was clearly visible that iron nanoparticles had started to present an orange color, typical of its oxidation.

4 Conclusions

In this study, very low current densities were used to enhance the transport of polymer-coated iron nanoparticles in different porous media, using high nZVI concentrations typical of field applications. Because of these conditions, some aggregation of the nanoparticles was observed, particularly near the injection point. Higher currents should be tested with these concentrations to check if the enhancement in transport compared to diffusion is proportional to the applied current as reported by other researchers. The experimental results show that the electrical field applied to clay-rich media enhances the ORP creating a synergistic

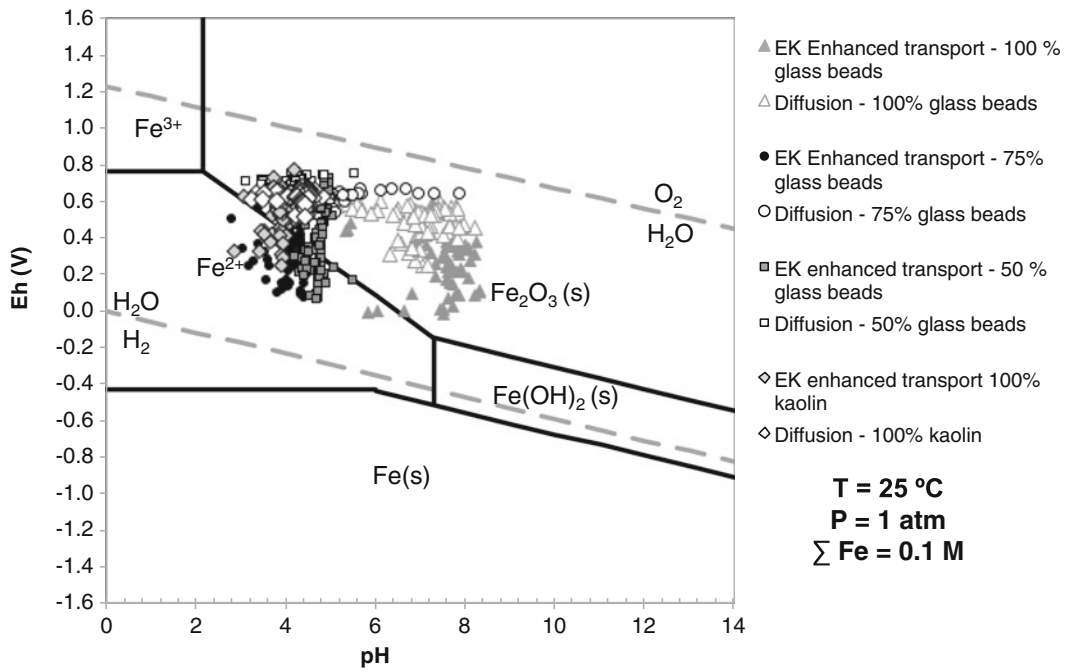

Fig. 10 Pourbaix diagram with the values measured during 48 h in the electrodes embedded in the electrophoretic cell

effect of nZVI usage with electrokinetics, delaying its corrosion reaction. This effect was also observed in earlier studies, where the ORP enhancement was attributed to the polarization of the diffuse double layer of the clay media.

The transport of polymer-stabilized iron nanoparticles can be enhanced by the direct current, in low permeability clay soils, where EOF can be effective in distributing the particles as well as electrophoretic mobility of the particles themselves. Further work is necessary for comprehensive treatise of the behavior of nZVI in clay-rich soils under direct current applications, namely the measuring of the EOF.

Acknowledgments This work has been funded by the European Regional Development Fund (ERDF) through COMPETE—Operational Program for Competitiveness Factors (OPCF), by Portuguese National funds through "FCT—Fundação para a Ciência e a Tecnologia" under project «PTDC/AGR-AAM/101643/2008 NanoDC», by the research grant SFRH/BD/76070/2011, by FP7-PEOPLE-IRSES-2010-269289-ELECTROACROSS and by RIARTAS-Red Iberoamericana de aprovechamiento de residuos industriales para el tratamiento de suelos y aguas contaminadas, Programa Iberoamericano de Ciencia y Tecnología para el Desarrollo (Cyted). The Department of Civil and Environmental Engineering at Lehigh University is acknowledged, where all the equipment development, testing, and analysis for this work were funded. Dan Zeroka is kindly acknowledged for the electrophoretic cell modification.

References

Bahranowski, K., Serwicka, E. M., Stoch, L., & Srycharski, P. (1993). On the possibility of removal of nonstructural iron from kaolinite-group minerals. *Clay Minerals, 28*, 379–391.

Bennett, P., He, F., Zhao, D., Aiken, B., & Feldman, L. (2010). In situ testing of metallic iron nanoparticle mobility and reactivity in a shallow granular aquifer. *Journal of Contaminant Hydrology, 116*(1–4), 35–46.

Chang, J.-H., & Cheng, S.-F. (2006). The remediation performance of a specific electrokinetics integrated with zerovalent metals for perchloroethylene-contaminated soils. *Journal of Hazardous Materials B, 131*, 153–162.

Chowdhury, A. I. A., O'Carroll, D. M., Xu, Y., & Sleep, B. E. (2012). Electrophoresis enhanced transport of nanoscale zerovalent iron. *Advances in Water Resources, 40*, 71–82.

Comba, S., Di Molfetta, A., & Sethi, R. (2011). A comparison between field applications of nano-, micro-, and millimetric zerovalent iron for the remediation of contaminated aquifers. *Water, Air, & Soil Pollution, 215*(1), 595–607.

Elliott, D. W., & Zhang, W. (2001). Field assessment of nanoscale bimetallic particles for groundwater treatment. *Environmental Science & Technology, 35*, 4922–4926.

He, F., Zhao, D., & Paul, C. (2010). Field assessment of carboxymethyl cellulose stabilized iron nanoparticles for in situ destruction of chlorinated solvents in source zones. *Water Research, 44*, 2360–2370.

Henn, K. W., & Waddill, D. W. (2006). Utilization of nanoscale zerovalent iron for source remediation—A case study. *Remediation, 16*(2), 57–77.

Jiemvarangkul, P. (2012). Nanoparticles for Nonaqueous-phase liquids (NAPLs) Remediation, Dissertation presented to the Graduate and Research Committee of Lehigh University for the Degree of Doctor of Philosophy in Environmental Engineering.

Jiemvarangkul, P., Zhang, W. X., & Lien, H. L. (2011). Enhanced transport of polyelectrolyte stabilized nanoscale zerovalent iron (nZVI) in porous media. *Chemical Engineering Journal, 170*(2–3), 482–491.

Jones, E. H., Reynolds, D. A., Wood, A. L., & Thomas, D. G. (2010). Use of electrophoresis for transporting nano-iron in porous media. *Ground Water, 49*(2), 172–183.

Kanel, S. R., Goswami, R. R., Clement, T. P., Barnett, M. O., & Zhao, D. (2008). Two-dimensional transport characteristics of surface stabilized zerovalent iron nanoparticles in porous media. *Environmental Science & Technology, 42*, 896–900.

Kim, H.-J., Phenrat, T., Tilton, R. D., & Lowry, G. V. (2012). Effect of kaolinite, silica fines, and pH on transport of polymer-modified zerovalent iron nanoparticles in heterogeneous porous media. *Journal of Colloid and Interface Science, 370*(1), 1–10.

Li, X., Elliott, D. W., & Zhang, W. (2006). Zerovalent iron nanoparticles for abatement of environmental pollutants: materials and engineering aspects. *Critical Reviews in Solid State and Materials Sciences, 31*(4), 111–122.

Lin, Y.-H., Tseng, H.-H., Wey, M.-Y., & Lin, M.-D. (2010). Characteristics of two types of stabilized nano zerovalent iron and transport in porous media. *Science of the Total Environment, 408*(10), 2260–2267.

Masciangioli, T., & Zhang, W. (2003). Environmental technologies at the nanoscale. *Environmental Science & Technology, 37*(5), 102A–108A.

Mehra, O. P., & Jackson, M. L. (1960). Iron oxide removal from soils and clays by a dithionite–citrate system buffered with sodium bicarbonate. *Clays and Clay Minerals, 7*, 317–327.

Noubactep, C., Caré, S., & Crane, R. (2012). Nanoscale metallic iron for environmental remediation: prospects and limitations. *Water, Air, & Soil Pollution, 223*(3), 1363–1382.

O'Hara, S., Krug, T., Quinn, J., Clausen, C., & Geiger, C. (2006). Field and laboratory evaluation of the treatment of DNAPL source zones using emulsified zerovalent iron. *Remediation, 16*(2), 35–56.

Pamukcu, S., Weeks, A., & Wittle, J. K. (2004). Enhanced reduction of Cr(VI) by direct electric current in a contaminted clay. *Environmental Science & Technology, 38*, 1236–1241.

Pamukcu, S., Hannum, L., & Wittle, J. K. (2008). Delivery and activation of nano-iron by DC electric field. *Journal of Environmental Science and Health, Part A, 43*(8), 934–944.

Phenrat, T., Saleh, N., Sirk, K., Tilton, R. D., & Lowry, G. V. (2007). Aggregation and sedimentation of aqueous nanoscale zerovalent iron dispersions. *Environmental Science & Technology, 41*, 284–290.

Phenrat, T., Kim, H.-J., Fagerlund, F., Illangasekare, T., Tilton, R. D., & Lowry, G. V. (2009). Particle size distribution, concentration, and magnetic attraction affect transport of polymer-modified Fe^0 nanoparticles in sand columns. *Environmental Science & Technology, 43*, 5079–5085.

Reddy, K. R., & Karri, M. R. Effect of electric potential on nanoiron particles delivery for pentachlorophenol remediation in low permeability soil. In M. Hamza et al. (Ed.), Proceedings of the 17th International Conference on Soil Mechanics and Geotechnical Engineering: The Academia and Practice of Geotechnical Engineering, Alexandria, Egypt, 5–9 October 2009, 2312–2315.

Reddy, K. R., Darko-Kagy, K., & Cameselle, C. (2011). Electrokinetic-enhanced transport of lactate-modified nanoscale iron particles for degradation of dinitrotoluene in clayey soils. *Separation and Purification Technology, 79*(2), 230–237.

Shi, Z., Nurmi, J. T., & Tratnyek, P. G. (2011). Effects of nano zerovalent iron on oxidation-reduction potential. *Environmental Science and Technology, 45*, 1586–1592.

Sun, Y.-P., Li, X., Cao, J., Zhang, W., & Wang, H. P. (2006). Characterization of zerovalent iron nanoparticles. *Advances in Colloid and Interface Science, 120*, 47–56.

USEPA (2011). Fact sheet on selected sites using or testing nanoparticles for remediation. United States Environmental Protection Agency. http://cluin.org/products/nanozvi/. Accessed 3 April 2012

Yang, G. C. C., & Yeh, C.-F. (2011). Enhanced nano-$Fe_3O_4/S_2O_8^{2-}$ oxidation of trichloroethylene in a clayey soil by electrokinetic. *Separation and Purification Technology, 79*, 264–271.

Yang, G. C. C., Tu, H.-C., & Hung, C.-H. (2007). Stability of nanoiron slurries and their transport in the subsurface environment. *Separation and Purification Technology, 58*, 166–172.

Yang, G. C. C., Hung, C.-H., & Tu, H.-C. (2008). Electrokinetically enhanced removal and degradation of nitrate in the subsurface using nanosized Pd/Fe slurry. *Journal of Environmental Science and Health, Part A, 43*(8), 945–951.

Yuan, S., Long, H., Xie, W., Liao, P., & Tong, M. (2012). Electrokinetic transport of CMC-stabilized Pd/Fe nanoparticles for the remediation of PCP-contaminated soil. *Geoderma, 185–186*, 18–25.

Zhang, W. (2003). Nanoscale iron particles for environmental remediation: an overview. *Journal of Nanoparticle Research, 5*, 323–332.